

Isotope effect in charge-transfer collisions of H with He⁺J. Loreau,¹ S. Ryabchenko,^{2,3} A. Dalgarno,¹ and N. Vaeck^{3,*}¹*Institute for Theoretical Atomic, Molecular and Optical Physics, Harvard-Smithsonian Center for Astrophysics, Cambridge, Massachusetts 02138, USA*²*Northern (Arctic) Federal University, 17 Severnaya Dvina Emb., 163002 Arkhangelsk, Russia*³*Laboratoire de Chimie Quantique et Photophysique, Université Libre de Bruxelles (ULB), CP160/09, 1050 Bruxelles, Belgium*
(Received 9 August 2011; published 22 November 2011)

We present a theoretical study of the isotope effect arising from the replacement of H by T in the charge-transfer collision $H(n=2) + He^+(1s)$ at low energy. Using a quasimolecular approach and a time-dependent wave-packet method, we compute the cross sections for the reaction including the effects of the nonadiabatic radial and rotational couplings. For $H(2s) + He^+(1s)$ collisions, we find a strong isotope effect at energies below 1 eV/amu for both singlet and triplet states. We find a much smaller isotopic dependence of the cross section for $H(2p) + He^+(1s)$ collisions in triplet states, and no isotope effect in singlet states. We explain the isotope effect on the basis of the potential energy curves and the nonadiabatic couplings, and we evaluate the importance of the isotope effect on the charge-transfer rate coefficients.

DOI: 10.1103/PhysRevA.84.052720

PACS number(s): 34.70.+e, 52.20.Hv

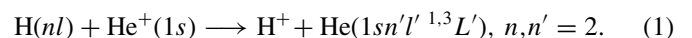
I. INTRODUCTION

Charge-transfer processes between atoms and ions are crucial in the study of astrophysical and laboratory plasmas. X-ray emission from solar system objects such as cometary and planetary atmospheres is due to a charge-transfer mechanism between solar wind ions and neutral atoms or molecules present in the atmospheres, while in the study of tokamak plasmas, charge exchange is used as a diagnostic tool via the observation of emission lines from impurity ions recombining with the plasma. In this respect, charge-transfer collisions between H and He⁺ ions are of particular importance. Helium ions form a significant fraction of the solar wind and can collide with the neutral hydrogen present in atmospheres, so that their interaction is important to model the production of far-ultraviolet radiation observed in the solar system. On the other hand, the plasma of a tokamak is composed of H (or rather of the heavier isotopes D and T) which fuse to form alpha particles. The helium ash can be considered an impurity, and the emission lines of He resulting from the charge transfer of He⁺ ions with hydrogen can be used in the diagnostic of the plasma [1].

In a recent work [2], the charge-transfer reaction between excited ($n = 2, 3$) hydrogen and He⁺(1s) in the energy range 0.25 – 150 eV/amu was studied using a fully quantal approach. This reaction is particularly important in the plasma edge region, as it modifies the population of the excited states of He, which are used to determine various plasma parameters [3]. While the population of the excited states is relatively small in a tokamak plasma [4], it is compensated by the fact that the cross section is expected to scale as n^4 . However, in the nuclear fusion process, the reaction fuel is not composed of hydrogen but of a mixture of deuterium and tritium. The different isotopes of hydrogen are usually not distinguished, as the isotope effect on charge-transfer cross sections is assumed to be very small [5], except at extremely low energies. It was suggested that at collisional energies much higher than the

isotope mass shift (0.0037 eV between H and D), the isotope effect should be negligible. However, Stancil and Zygelman [6] later showed that an isotope effect could occur at energies as high as 10 eV/amu in $N^{4+} + H(D)$ collisions. These authors interpreted this effect with the Landau-Zener-Stueckelberg model and suggested that it could occur at energies as high as 1 keV/amu for some systems. Moreover, it was established that the cross section decreases with increasing system reduced mass [7], a behavior that has since been observed in other charge-transfer collisions [8,9]. Recently, Stolterfoht *et al.* [10,11] observed a very important isotope effect in collisions between He²⁺ and H, the replacement of H by D or T leading to a variation of the cross section for energies as high as 300 eV/amu. For this system the cross section was found to increase with the reduced mass of the system, and the isotope effect was attributed to the importance of the nonadiabatic rotational couplings in the small impact parameter region.

This motivates an investigation of the isotope effect on the charge-transfer cross sections in $H(nl) + He^+(1s)$ collisions. We focus here on the charge transfer in the $n = 2$ manifold of H and He at low energy, which can occur in singlet or triplet states:



To study reaction (1), we use a quasimolecular approach to the ion-atom collision. We exploit quantum chemistry *ab initio* methods to obtain the potential energy curves as well as the nonadiabatic radial and rotational coupling matrix elements of the molecular ion HeH⁺. A time-dependent wave-packet method is then applied to treat the curve-crossing dynamics resulting from the failure of the Born-Oppenheimer approximation. The collision matrix elements are computed from an analysis of the flux in the asymptotic region by using properties of absorbing potentials, giving access to the charge-transfer cross sections. Due to the close spacing between the electronic states as well as the alternation between states dissociating into $H(nl) + He^+(1s)$ or $H^+ + He(1snl \ ^{1,3}L)$

*nvaeck@ulb.ac.be

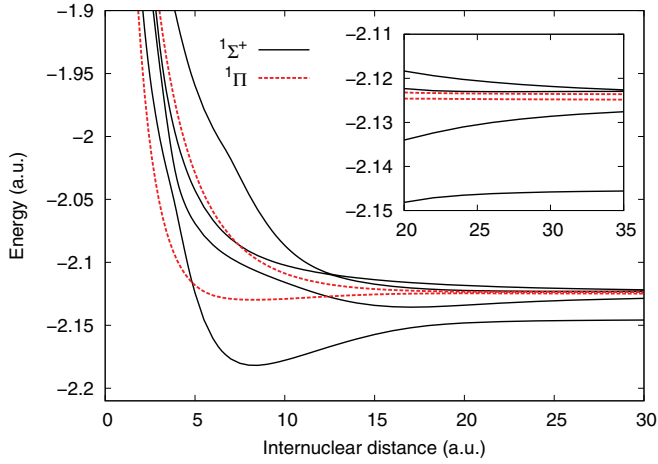


FIG. 1. (Color online) Adiabatic PEC's of the $n = 2$ singlet states of HeH^+ . Solid lines, $^1\Sigma^+$ states. Dotted lines, $^1\Pi$ states.

along the spectrum, this system provides an illustration of different types of isotope effects that arise in charge-transfer collisions at low energy.

II. THEORETICAL METHOD

The entrance channel in reaction (1) can be either a singlet or a triplet state. Accordingly, it is necessary to compute the potential energy curves (PEC's) of the HeH^+ molecular ion, as well as the nonadiabatic couplings, in both spin multiplicities. For $n = 2$, this amounts to a total of 12 states, which have been studied previously [12,13]. We reproduce the potential energy curves of these states in Figs. 1 and 2 and their dissociation products in Table I, as we will need them to support the discussion of our results. Note that asymptotically, the fifth and sixth $^1\Sigma^+$ states correspond, respectively, to $\text{H}(2s) + \text{He}^+(1s)$ and $\text{H}^+ + \text{He}(1s2p\ ^1P^o)$. However, these two states effectively cross at an internuclear distance of 50 a.u. due to the Stark effect (see Ref. [12], and in particular Fig. 4, for details), so that in the interaction region the order of these two states is reversed. We do not consider the three $n = 1$ states (two $^1\Sigma^+$ states and one $^3\Sigma^+$ state), as they

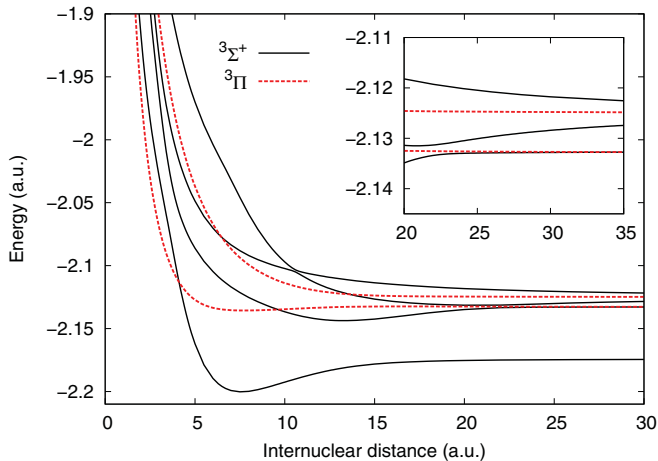


FIG. 2. (Color online) Adiabatic PEC's of the $n = 2$ triplet states of HeH^+ . Solid lines, $^3\Sigma^+$ states. Dotted lines, $^3\Pi$ states.

TABLE I. $n = 2$ states of the HeH^+ molecular ion and their dissociation products. m is used to number the states for a given value of Λ and S . The $n = 1$ states (two $^1\Sigma^+$ states and one $^3\Sigma^+$ state) are not included.

$2S+1\Lambda$	m	Atomic products	
$^1\Sigma^+$	3	$\text{H}^+ + \text{He}(1s2s\ ^1S)$	
	4	$\text{H}(2p) + \text{He}^+(1s)$	
	5	$\text{H}(2s) + \text{He}^+(1s)$	
	6	$\text{H}^+ + \text{He}(1s2p\ ^1P^o)$	
	$^1\Pi$	1	$\text{H}(2p) + \text{He}^+(1s)$
		2	$\text{H}^+ + \text{He}(1s2p\ ^1P^o)$
$^3\Sigma^+$		2	$\text{H}^+ + \text{He}(1s2s\ ^3S)$
	3	$\text{H}^+ + \text{He}(1s2p\ ^3P^o)$	
	4	$\text{H}(2p) + \text{He}^+(1s)$	
	5	$\text{H}(2s) + \text{He}^+(1s)$	
$^3\Pi$	1	$\text{H}^+ + \text{He}(1s2p\ ^3P^o)$	
	2	$\text{H}(2p) + \text{He}^+(1s)$	

are much lower in energy and thus not expected to give a significant contribution to the cross section. Moreover, it was previously shown [2] that it is not necessary to include the $n = 3$ manifold to get an accurate description of the charge-transfer reaction (1) involving $n = 2$ states, so we will neglect them in our calculations. The adiabatic PEC's for these states have been calculated at the state-averaged complete active space self-consistent field and configuration interaction levels using the *ab initio* quantum chemistry package MOLPRO version 2006.1 [14]. An adapted basis set consisting of the aug-cc-pv5Z basis set [15] supplemented by one contracted Gaussian function per orbital per atom has been used. Details of the molecular structure calculations can be found in [12].

This approach allows us to compute the nonadiabatic radial couplings $F_{mm'}$, which govern the charge-transfer process. The nonadiabatic radial couplings are the matrix elements of the operator ∂_R in the basis of the adiabatic electronic functions $\{\zeta_m\}$: $F_{mm'} = \langle \zeta_m | \partial_R | \zeta_{m'} \rangle$. The dominant nonadiabatic radial couplings are shown in Fig. 3 for the singlet states and in Fig. 4 for the triplet states. As can be expected, these are the

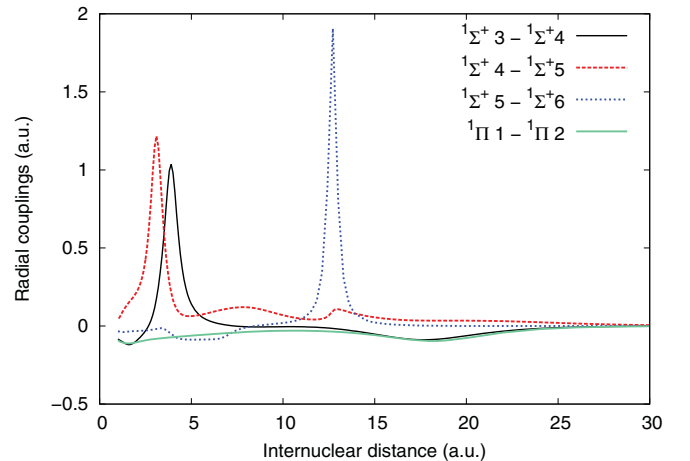


FIG. 3. (Color online) Principal radial nonadiabatic coupling matrix elements between the $n = 2$ singlet states of HeH^+ .

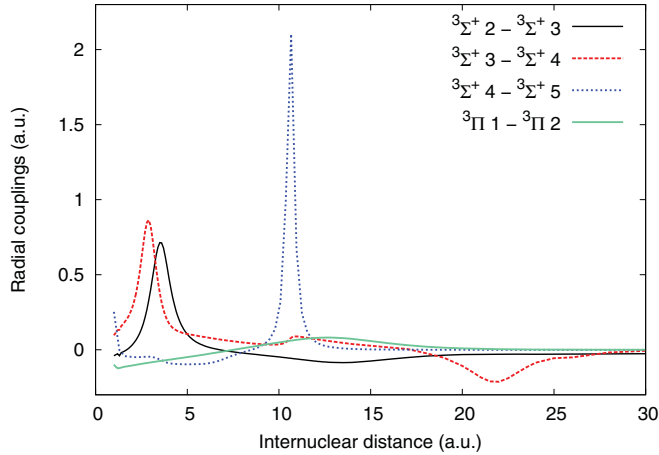


FIG. 4. (Color online) Principal radial nonadiabatic coupling matrix elements between the $n = 2$ triplet states of HeH^+ .

couplings between adjacent states, $F_{m,m\pm 1}$. The position of the maximum of the couplings corresponds to the position of the avoided crossings that can be observed in Figs. 1 and 2. We also included in our calculations the nonadiabatic rotational couplings, which are the matrix elements of the operator L_y and connect states with $\Delta\Lambda = 1$.

The cross section corresponding to the transfer of an electron from an initial state ℓ to a final state ℓ' (where the index ℓ is shorthand for all the quantum numbers necessary to describe the electronic states; in this case ℓ stands for $mS\Lambda$) is given by a sum over the rotational quantum number K of the S matrix elements $S_{\ell'\ell}^K(E)$ [16]:

$$\sigma_{\ell',\ell}(E) = \frac{\pi}{k_\ell^2(E)} \sum_K (2K+1) |S_{\ell'\ell}^K(E) - \delta_{\ell'\ell}|^2, \quad (2)$$

where k_ℓ is the wave number in the entrance channel, $k_\ell = \{2\mu[E - U_\ell(\infty)]\}^{1/2}$, and $U_\ell(R)$ is the corresponding adiabatic potential energy curve. In this work, the S -matrix elements are calculated by a fully quantal time-dependent wave-packet method. This approach has been described previously [2,17–19], and we will only recall its main features. We start by defining a Gaussian wave packet on the initial state. This wave packet is then propagated on the potential energy curves coupled by the nonadiabatic radial and rotational couplings. The time propagation is done using the split operator algorithm [20], which requires the knowledge of the diabatic representation. For each value of K , the scattering matrix elements $|S_{\ell'\ell}^K(E)|^2$ are then extracted from the wave packet on each electronic state using the flux operator formalism with a complex absorbing potential [21].

At very low energy (below 0.5 eV), we confirmed the validity of our results by using a time-independent approach.

III. RESULTS AND DISCUSSION

A. Charge transfer in $\text{H}(2s) + \text{He}^+(1s)$ collisions

The spin-dependent cross sections for the electron capture from $\text{H}(2s)$ by $\text{He}^+(1s)$ and summed over the final states are presented in Fig. 5 as a function of the energy of collision.

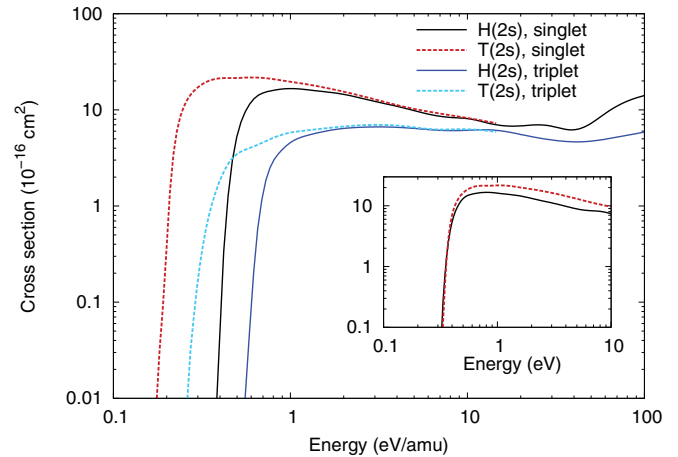


FIG. 5. (Color online) Cross sections for the charge-transfer reaction $[\text{H},\text{T}](2s) + \text{He}^+(1s) \rightarrow [\text{H},\text{T}]^+ + \text{He}(1s2l \ ^1,^3L)$ in the laboratory frame. The inset shows the cross section for the singlet manifold in the center-of-mass frame.

We have also plotted, in the same figure, the cross sections obtained when H is replaced by T.

We first note that at energies below 5 eV/amu, the reaction is dominated by capture in the singlet states. Despite this, the cross section presents the same behavior in both spin multiplicities, decreasing very quickly at energies below 1 eV/amu (≈ 0.5 eV/amu for singlet states and ≈ 0.7 eV/amu for triplet states). This is precisely the energy at which the isotope effect starts to appear. The cross sections for T are seen to decrease as quickly as for H, but shifted to a lower energy (≈ 0.2 eV/amu for singlet states and ≈ 0.3 eV/amu for triplet states). Therefore, we observe a strong isotope effect and the ratio of the cross sections $\sigma_{\text{T}}/\sigma_{\text{H}}$ reaches a factor as large as 10^3 . The isotope effect is of the same nature in both spin multiplicities, *i.e.*, an increase of the cross section with the reduced nuclear mass. It can be explained on the basis of the PEC's and nonadiabatic radial couplings. The transition $\text{H}(2s) + \text{He}^+(1s) \rightarrow \text{H}^+ + \text{He}(1s2p \ ^1P^0)$, which dominates the charge transfer of the $2s$ electron at low energy, corresponds to the transition between the fifth and sixth $^1\Sigma^+$ states. This transition is driven by the radial coupling F_{56} , which peaks at an internuclear distance $R_c = 12.7$ a.u., corresponding to the avoided crossing between the two PEC's (see Figs. 1 and 3). This crossing occurs in the repulsive region of the potential, at an energy of $V(R_c) = 0.39$ eV above the asymptotic energy of the entrance channel. This leads to the threshold condition $E > V(R_c)$, where $V(R) = U(R) + K(K+1)/2\mu R^2$ is the electronic energy in the entrance channel and R_c is the location of the avoided crossing. For energies below this threshold, the avoided crossing is not reachable and the transition probability decreases exponentially. In the center-of-mass frame, the threshold energy $E = V(R_c)$ is the same for H and T, as illustrated in the inset of Fig. 5, although for singlet states the peak of the cross section (at an energy of 1 eV) is larger for T than for H by about 25%. However, when transformed in eV/amu, the cross section is inversely proportional to the reduced mass μ so that the threshold is shifted down to lower energies for T due to the larger reduced mass. As a result, we observe a huge isotope effect below 0.5 eV/amu.

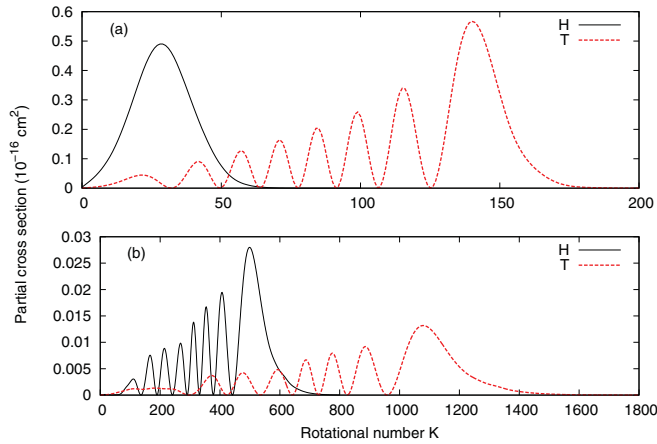


FIG. 6. (Color online) Partial cross sections as a function of K for the capture into $\text{He}(1s2p\ ^1P^0)$ from the $2s$ state of H (solid line) or T (dotted line) in the $^1\Sigma^+$ states. (a) $E = 0.6$ eV/amu, (b) $E = 25$ eV/amu.

We further investigate the isotope effect by examining the partial cross sections as a function of K . This is illustrated in Fig. 6 for the capture of the $2s$ electron of H or T into $\text{He}(1s2p\ ^1P^0)$ in the $^1\Sigma^+$ states. This is the transition that dominates the capture from the $2s$ state in the singlet states and which is responsible for the isotope effect at low energy. For a given energy, the range of values of K is much larger for T than for H. At $E = 0.6$ eV/amu, we observe only one peak in the partial cross section for H, while for T we observe eight peaks, the last one being as large as the single peak of H. It is therefore clear that the total cross section will be enhanced for T. At $E = 25$ eV/amu, however, the partial cross section is composed of eight peaks for both isotopes. The peaks become wider as the reduced mass increases, but at the same time their intensity is reduced. In this case, the net result is that the cross section is mass-independent. As the transition becomes negligible below the threshold energy, the maximum value of the rotational quantum number K appearing in the sum in Eq. (2) can be easily estimated by solving $E = U(R_c) + K_{\max}(K_{\max} + 1)/2\mu R_c^2$ with $R_c = 12.7$ a.u. and $U(R_c) = 0.39$ eV. For $E = 0.6$ eV/amu, we get $K_{\max} = 39$ for H and $K_{\max} = 155$ for T while for $E = 25$ eV/amu, we get $K_{\max} = 584$ for H and $K_{\max} = 1263$ for T, which agrees with Figs. 6(a) and 6(b).

The isotope effect in the triplet states is of the same nature. The capture of the $2s$ electron is dominated by the state $\text{He}(1s2p\ ^3P^0)$ at low energy. As can be seen from Table I, this is not a direct transition, in the sense that the electronic states are not adjacent: $\text{H}(2s) + \text{He}^+(1s)$ correlates with the fifth $^3\Sigma^+$ state, while $\text{H}^+ + \text{He}(1s2p\ ^3P^0)$ corresponds to the third $^3\Sigma^+$ state. Since the radial coupling between these states is small, the reaction occurs mainly through the coupling of these states with the fourth $^3\Sigma^+$ state, which dissociates into $\text{H}(2p) + \text{He}^+(1s)$. This constitutes a two-step process which will be governed by the radial couplings F_{45} and F_{34} , shown in Fig. 4. The radial coupling F_{45} peaks at $R = 10.8$ a.u., corresponding to the avoided crossing between the two PEC's (see Fig. 2). This avoided crossing occurs in the repulsive region, at an energy about 0.52 eV above the asymptotic energy

of the entrance channel. If the energy of collision is below this threshold, it is thus expected that the transition probability to the $4\ ^3\Sigma^+$ state, and therefore also to the $3\ ^3\Sigma^+$ state, will become very small. Correspondingly, and as in the case of singlet states, the charge-transfer cross section shows a very rapid decrease when the center-of-mass energy is smaller than 0.52 eV.

B. Charge transfer in $\text{H}(2p) + \text{He}^+(1s)$ collisions

The cross sections for capture from $\text{H}(2p)$ by $\text{He}^+(1s)$ for singlet and triplet states are presented in Fig. 7. We observe that at energies above 30 eV/amu, the cross sections for both spin multiplicities are equal. At lower energy, the cross section for singlet states decreases much faster than for triplet states, so that the charge-transfer process will be dominated by capture into the triplet states. This contrasts with the capture from $\text{H}(2s)$, which is dominated by singlet states at low energy. Moreover, the cross sections for capture from $\text{H}(2p)$ do not present any threshold as a function of the energy of collision, as the avoided crossings controlling the charge-transfer reaction occur in the attractive region of the potential energy curves.

The isotope effect for singlet and triplet states is found to be very different. For singlet states, the cross sections for H and T in the laboratory frame are essentially identical. The charge transfer is dominated at low energy by capture into $\text{H}^+ + \text{He}(1s2p\ ^1P^0)$ in the $^1\Pi$ states. The particularity of this transition is that it is governed by a very small and wide radial coupling between two PEC's that are nearly degenerate at dissociation (see Figs. 1 and 3), leading to parallel diabatic curves, which can be described using the Rosen-Zener-Demkov model [22]. In the center-of-mass frame, the cross section for T is therefore much smaller than for H, as shown in the inset of Fig. 7. This is important, as it is often assumed that the cross sections for different isotopes are very similar in the center-of-mass frame. Therefore, very few calculations are performed for the different isotopes of atoms involved in charge-transfer reactions, the cross section being simply obtained in the laboratory frame by scaling the results

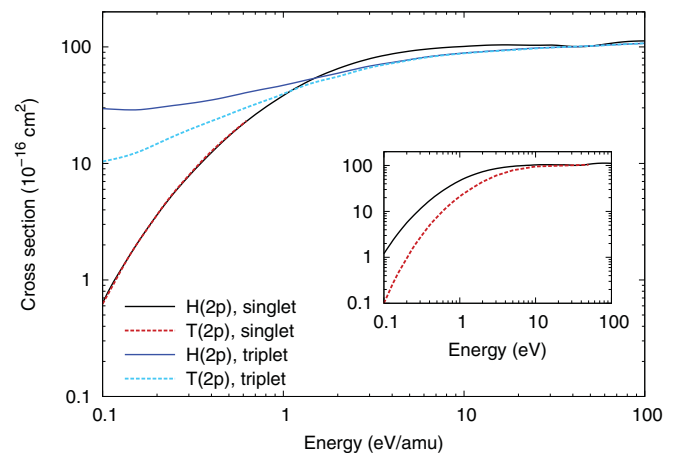


FIG. 7. (Color online) Cross sections for the charge-transfer reaction $[\text{H},\text{T}](2p) + \text{He}^+(1s) \rightarrow [\text{H},\text{T}]^+ + \text{He}(1s2l\ ^1,^3L)$ in the laboratory frame. The inset shows the cross section for the singlet manifold in the center-of-mass frame.

for the more abundant of them. In the case of the singlet charge-transfer reaction $\text{H}(2p) + \text{He}^+(1s)$, this simplified approach would result in an error on the cross section of a factor of 2 at 1 eV/amu and an order of magnitude at 0.1 eV/amu.

On the other hand, for triplet states there is an isotope effect that takes place at energies below 3 eV/amu. In addition, the effect is reversed compared to the capture from the $2s$ state as the charge-transfer cross section decreases with an increase in the reduced mass. We also see that the effect is much smaller than for the $2s$ state of H: the largest ratio $\sigma_{\text{H}}/\sigma_{\text{T}}$, which occurs at the lowest energy considered (0.1 eV/amu), is about 3. This isotope effect is similar to the one first studied by Stancil and Zygelman [6] using the Landau-Zener approximation and recently discussed by Barragán *et al.* [23]. In these cases, the avoided crossings at which the charge transfer occurs are located at large internuclear distances, where the potential is attractive. In the case of the charge transfer from $\text{H}(2p)$ in the triplet states, the reaction is dominated at low energy by the capture into $\text{He}(1s2p\ ^3P^o)$ in the Σ states, corresponding to the transition between the fourth and third $^3\Sigma^+$ states. These states undergo two avoided crossings: one in the repulsive region of the potential at an internuclear distance $R = 2.9$ a.u., and a second one in the attractive region at $R = 21.8$ a.u. (see Fig. 4 and the inset of Fig. 2). At low energy, the first avoided crossing is inaccessible, and the transition occurs through the second, wider coupling. In this case, we still observe wider peaks in the partial cross section for T than for H, but the magnitude of the peaks is much smaller for the heavier isotope at low energy, resulting in a decrease of the cross section. This behavior of the partial cross sections has been observed in other systems such as $\text{N}^{4+} + \text{H}$ [7] or $\text{Si}^{4+} + \text{He}$ [24].

Finally, we computed the cross section with and without the rotational couplings in order to estimate their effect, and found the effect to be negligible. This was expected, as it was previously shown for $\text{H} + \text{He}^+$ collisions that these couplings do not modify the state-to-state cross sections below 1 eV/amu, where the isotope effect takes place [2]. This confirms that for this system, the rotational couplings do not bring an additional isotope effect, as opposed to what was observed in collisions of He^{2+} and other light ions with H [11,25].

C. Rate coefficients

Although the isotope effect only appears at low energies, it can significantly affect the charge-transfer reaction rate at high temperatures. If we assume a Maxwell-Boltzmann distribution of the energy of the colliding particles, the rate coefficient is given by

$$k(T) = \left(\frac{2}{k_B T}\right)^{3/2} \frac{1}{\sqrt{\pi\mu}} \int_0^\infty E e^{-E/k_B T} \sigma(E) dE, \quad (3)$$

where k_B is the Boltzmann constant. As an example, we have plotted in Fig. 8 the rate coefficient of the charge-transfer reactions $\text{H}(2s) + \text{He}^+(1s) \rightarrow \text{H}^+ + \text{He}(1s2l)$ in the singlet states and $\text{H}(2p) + \text{He}^+(1s) \rightarrow \text{H}^+ + \text{He}(1s2l)$ in the triplet states, as well as the same rate coefficients when H is replaced

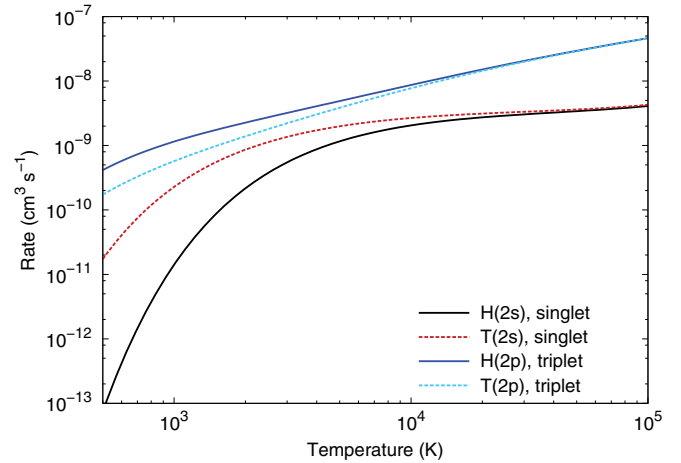


FIG. 8. (Color online) Isotope effect on the rate coefficient for the capture of the $2s$ electron of $\text{H}(\text{T})$ in the singlet states and of the $2p$ electron of $\text{H}(\text{T})$ in the triplet states as a function of the temperature.

by T. We observe that isotope effects can be expected for temperatures as high as 10 000 K.

IV. CONCLUSIONS

Using a time-dependent wave-packet propagation method, we investigated the isotopic dependence of the charge-transfer cross sections for the collisions $\text{H}(n = 2) + \text{He}^+(1s)$ when H is replaced by T. In $\text{H}(2s) + \text{He}^+(1s)$ collisions, we found a very strong isotope effect at energies below 1 eV/amu. For both singlet and triplet states, the cross section increases with increasing reduced mass, which is due to the fact that the exit channels become closed at low energy as the nonadiabatic couplings responsible for the transition are located in the repulsive region of the potential energy curves. This threshold energy in the center-of-mass frame results in a large isotope effect when transformed in the laboratory frame. In $\text{H}(2p) + \text{He}^+(1s)$ collisions, we found a different behavior of the cross section for singlet and triplet states. For the former we did not observe any isotope effect, while for the latter we observed an isotope effect at energies below 3 eV/amu, the cross section decreasing with increasing reduced mass. We also showed that the isotope effect influences the charge-transfer rate coefficients at temperatures as high as 10^4 K.

The reaction studied provides examples of various cases that can arise in the description of the isotope effect at low energy. To be able to determine the isotope effect, it is necessary to have detailed knowledge of the interaction potentials and of the nonadiabatic couplings of the system.

ACKNOWLEDGMENTS

J.L. acknowledges the support of the Belgian American Educational Foundation. N.V. acknowledges financial support from the ARC (ATMOS), IISN, and FRFC programs from the F.R.S.-FNRS.

- [1] F. B. Rosmej, R. Stamm, and V. S. Lisita, *Europhys. Lett.* **73**, 342 (2006).
- [2] J. Loreau, K. Sodoga, D. Lauvergnat, M. Desouter-Lecomte, and N. Vaeck, *Phys. Rev. A* **82**, 012708 (2010).
- [3] G. Bertschinger and O. Marchuk, in *Nuclear Fusion Research: Understanding Plasma-Surface Interactions*, edited by R. E. H. Clark and D. H. Reiter (Springer-Verlag, Berlin, Heidelberg, 2005), Chap. 8.
- [4] J. E. Rice, E. S. Marmar, J. L. Terry, E. Källne, and J. Källne, *Phys. Rev. Lett.* **56**, 50 (1986).
- [5] J. B. Delos, *Rev. Mod. Phys.* **53**, 287 (1981).
- [6] P. C. Stancil and B. Zygelman, *Phys. Rev. Lett.* **75**, 1495 (1995).
- [7] P. C. Stancil, B. Zygelman, N. J. Clarke, and D. L. Cooper, *J. Phys. B* **30**, 1013 (1997).
- [8] M. Pieksma, M. Gargaud, R. McCarroll, and C. C. Havener, *Phys. Rev. A* **54**, R13 (1996).
- [9] P. Barragán, L. F. Errea, L. Mendez, I. Rabadán, and A. Riera, *J. Phys. B* **41**, 225202 (2008).
- [10] N. Stolterfoht, R. Cabrera-Trujillo, Y. Öhrn, E. Deumens, R. Hoekstra, and J. R. Sabin, *Phys. Rev. Lett.* **99**, 103201 (2007).
- [11] N. Stolterfoht, R. Cabrera-Trujillo, P. S. Krstic, R. Hoekstra, Y. Öhrn, E. Deumens, and J. R. Sabin, *Phys. Rev. A* **81**, 052704 (2010).
- [12] J. Loreau, P. Palmeri, P. Quinet, J. Liévin, and N. Vaeck, *J. Phys. B* **43**, 065101 (2010).
- [13] J. Loreau, J. Liévin, and N. Vaeck, *J. Chem. Phys.* **133**, 114302 (2010).
- [14] H.-J. Werner, P. J. Knowles, R. Lindh, F. R. Manby, M. Schütz, P. Celani, T. Korona, G. Rauhut, R. D. Amos, A. B. A. Berning, D. L. Cooper, M. J. O. Deegan, A. J. Dobbyn, F. Eckert, C. Hampel, G. Hetzer, A. W. Lloyd, S. J. McNicholas, W. Meyer, M. E. Mura, A. Nicklaß, P. Palmieri, R. Pitzer, U. Schumann, H. Stoll, A. J. Stone, R. Tarroni, and T. Thorsteinsson, MOLPRO 2006.1, a package of *ab initio* programs.
- [15] T. H. Dunning Jr., *J. Chem. Phys.* **90**, 1007 (1989).
- [16] M. S. Child, *Molecular Collision Theory* (Academic, London, 1974).
- [17] N. Vaeck, M. Desouter-Lecomte, and J. Liévin, *J. Phys. B* **32**, 409 (1999).
- [18] N. Vaeck, M.-C. Bacchus-Montabonel, E. Baloïtcha, and M. Desouter-Lecomte, *Phys. Rev. A* **63**, 042704 (2001).
- [19] E. Baloïtcha, M. Desouter-Lecomte, M.-C. Bacchus-Montabonel, and N. Vaeck, *J. Chem. Phys.* **114**, 8741 (2001).
- [20] M. D. Feit, J. A. Fleck Jr., and A. Steiger, *J. Comput. Phys.* **47**, 412 (1982).
- [21] A. Jäckle and H.-D. Meyer, *J. Chem. Phys.* **105**, 6778 (1996).
- [22] Yu. N. Demkov, *Sov. Phys. JETP* **18**, 138 (1964).
- [23] P. Barragán, L. F. Errea, L. Mendez, and I. Rabadán, *Phys. Rev. A* **82**, 030701 (2010).
- [24] P. C. Stancil, B. Zygelman, N. J. Clarke, and D. L. Cooper, *Phys. Rev. A* **55**, 1064 (1997).
- [25] I. Y. Tolstikhina, D. Kato, and V. P. Shevelko, *Phys. Rev. A* **84**, 012706 (2011).